Library Progress International *Print version ISSN 0970 1052*
Vol.44, No.2s, Jul-Dec 2024: P.2040-2052 *Online version ISSN 2320 317X*

Original Article *Available online at www.bpasjournals.com*

Study of optical UV absorption and optical band gap determination of polyaniline with CdO

[1*]Ramabai N, [2,] Dr. Basavaraj Sannakki

[,] Department of Physics, SSA GFGC (A), BALLARI-583101, Karnataka State, India.
[and 2] Department of Physics, Gulbarga University, KALABURAGI-585106, Karnataka State, India.
Corresponding Author: ramabaissagfgc@gmail.com

How to cite this article: Ramabai N, Basavaraj Sannakki (2024). Study of optical UV absorption and optical band gap determination of polyaniline with CdO. *Library Progress International,* 44(2), 2040-2052

Abstract: In this investigation, the chemical oxidative polymerisation procedure was employed to synthesise the polymer polyaniline (PANI). Utilizing an UV-visible double beam spectrophotometer working in the 300-900 nm spectral district, the optical qualities of pure PANI orchestrated and PANI/CdO nanocomposite films with changing weight rates of Cadmium oxide (1% and 5%) were analyzed in two models, both when doping. The first results demonstrate that optical characteristics such as reflectance, optical conductivity, extinction coefficient, dielectric constants, refractive coefficient and absorption coefficient increased along with the expansion of the cadmium oxide (CdO) grouping. Moreover, the results demonstrate that for the direct allowed modification, the transmittance and optical energy gap upsides decreased from 4.41 to 4.12 eV with increasing doping percentages.

Keywords: *Band gap, UV absorption, Cadmium Oxide, Polyaniline, wavelength, Reflectance*

1. INTRODUCTION

Because of their better electrical, optical capabilities, thermal, dielectric and mechanical over other traditional materials, flexible composite materials are becoming more and more common in the utilisation of optical energy [1-2]. Because they are easily handled and pliable, polymer composites are nowadays very common in many uses for energy [3]. Clarifying polymers' optical properties and improving their application in optical energy uses have taken a lot of work [4]. Presently, there has been a lot of interest in using nanocomposite substances in academic and industrial settings [5–6]. This is because the overall performance of the polymeric materials could be enhanced by a tiny amount of the nano-additives. This can be attributed to the nanomaterials' high interfacial contact, large specific area, small size, and quantum confinement effects [7].

Interactions between conducting polymers and inorganic semiconductors can result in interesting properties that are very different from the individual components' properties [8]. The development of smart materials for use in next-generation technologies has given rise to a new field focused on conducting polymer nanostructures and nanocomposites [9–10]. It is thought to be simple to prepare and design nanocomposites where delocalized π-electrons can interact with inorganic nanoparticles to produce materials with special or improved properties by blending or encapsulating them in an intrinsically conducting polymer matrix [11]. In an effort to create novel, cutting-edge materials with enhanced mechanical, electrical, optical, and catalytic capabilities or to enhance the conduction mechanism in electronic devices, numerous studies on the manufacture of polymer nanocomposite have

been published. A wide variety of electrical and nanoelectronic devices have made use of these materials.

Wide band gap semiconductors' excellent optical transparency, adjustable carrier concentration, and customisable electrical conductivity make them crucial for today's electronics and energy applications. Tin-doped indium oxide, cadmium oxide, and zinc oxide are examples of transparent conductive oxides (TCOs), which are the semiconductors with broad band gaps that have been, studied the most. are crucial for numerous applications, including transparent conducting electrodes, surface acoustic wave devices, solar cells, phototransistor, diodes, and sensors, in addition to flat panel displays and optical communications. Excellent optical and electrical qualities are needed for these applications [12-13].

Ongoing research and development has been directed on conducting polymers because of their potential applications in numerous technological domains. Conducting polymers may provide a new class of polymers that combined the electrical and optical properties of metals or semiconductors with the mechanical and chemical processing benefits of polymers, offering enormous promise for a wide range of industrial applications [14]. PANI is one of the polymers used in optical energy uses. Because of PANI's UV radiation resistance, ultrafast responsiveness, electrical conductivity, consistent , ease of relative processing and flexibility it has been extensively explored as a nonlinear optical (NLO) material [15]. PANI, however, has restricted solubility, fusibility, and mechanical qualities. It must therefore be altered using different materials in order to overcome these drawbacks and expand its applications, particularly in the energy sector.

Because of its straightforward doping/dedoping chemistry, environmental stability, and ease of production, polyaniline (PANI) stands out among the family of conducting polymers. One of the conducting polymers that have been explored the most in the last 20 years is polyaniline, owing to its rich chemistry. Because it may be doped with organic dopants to increase its intrinsic electrical conductivity, PANI is a promising material [16]. Electrical conductivity akin to metal is anticipated in highly ordered structures, such as crystalline or self-assembled structures of perfect conducting polymers with p-conjugated structure. Additional elements serving as filler for the composite are needed to create an ordered structure [17–20]. The nanostructure of conducting polymers and their combined structure is a new field of study and research that aims to create novel materials for usage in both established and emerging industries. Because conducting polymer/metal oxide nanoparticle combinations offer better properties than either material alone, they have recently come to be recognised as a distinct class of materials.

An n-type semiconductor called cadmium oxide (CdO) is utilised as a transparent conductive material that is made into a transparent conducting film back. Applications for cadmium oxide include liquid crystal displays, anti-reflection coats, IR detectors, transparent electrodes, phototransistors and photovoltaic cells. When exposed to UV-A radiation, CdO micro particles experience band gap stimulation and preferentially degrade phenol. In light of CdO's many uses, it was deemed appropriate to employ nanoscale CdO as an inorganic substitute in the composite synthesis. In recent times, doped polymers have garnered attention from researchers doing both theoretical and experimental studies. This is because doping can provide the physical and chemical properties required for a particular application.

2. LITERATURE REVIEW

2.1. Optical Characteristics

Thin film optical characterization yields details regarding active optical defects, band structure, energy gap, band gap, and so forth. From transmission or absorbance, the optical band gap (Eg) and absorption coefficient can be determined. The Swanepoel approach can be used to calculate the film thickness (t) and refractive index from the absorbance spectrum [21, 22].The absorption coefficient is referred to the imaginary component of the refractive index (n) complex, also known as the extinction coefficient k.

Chemical interactions between analyte molecules and polyaniline-based coatings give rise to the measurement of polyaniline's optical characteristics in sensor applications. The refractive index, thickness, and optical absorbance spectrum are all affected by these measurements. The optical sensor's sensitivity, selectivity, and response are shown by changes in these optical properties [23]. However, it frequently gets challenging due to the appearance of some solutions to obtain a ballpark estimate of the thickness t and refractive index n.

2.2. Polyaniline Polymer

Polyaniline (PANI), previously known as dark aniline, can take on a few structures relying upon the level of oxidation. In addition, PANI is notable for its ecological soundness, doping potential with protonic acids, and effortlessness [24]. By connecting the 1-4 coupling of the aniline monomer elements, PANI can be discovered. PANI is present in a range of oxidation states and can be recognised by FTIR benzenoid to quinonoid ratios.

Forming conductive polymers is mostly made up of polythiophene (PTH), polypyrrole (PPY), polyaniline (PANI), and their byproducts [25, 26]. Electromagnetic impedance safeguarding, photothermal treatment, gas division layer, photovoltaic cell, battery-powered battery, synthetic sensor, hostile to erosion covering, microwave retention, and a lot more potential purposes are workable for them [27]. Conductive polymers are also used to obtain leading polymer compounds; for instance, they are directed fillers in polymer substrate protection [28–29]. These substances have expected involves in electronic gear, boundaries against electromagnetic impedance, and terminals for shows [30].

While conductive polymers — PANI specifically — offer various extraordinary advantages, they likewise have various downsides. For example, PANI's low handling limit, inflexibility, and absence of biodegradability limit its organic applications. The unbending spine's adverse consequences for PANI's poor dissolvability are the essential issue [31]. Numerous methods have been attempted to improve its processability; two major efforts to get over these problems include synthetic changes, namely the utilisation of substitute PANI subordinates and doped PANI. When contrasted with pure PANI, the chemically modified PANI shows better conductivity and anti-corrosion qualities as well as better handling qualities.

2.3. PANI-CdO nanocomposites: synthesis

In-situ polymerisation was used to create the PANI-CdO nanocomposite [32]. The first step in the polymerisation of monomer aniline was to add APS dropwise to an acidic solution containing a predetermined amount of synthetic CdO powder. After two hours of vigorous stirring, the solution was left overnight. The mixture was filtered the following day, cleaned with methanol and distilled water, and let to dry overnight at 80ºC.

3. METHODOLOGY

The following raw materials were utilised to make the samples: The synthesis of CdO nanoparticles involved the calcination of Cd(OH)2 nanoparticles, which served as precursors and were created using an arc discharge process in deionised water. PANI was created by the chemical oxidative polymerisation technique, which is comparable to the procedure described in [33]. Pure PANI was produced by diluting 2.59 g of aniline hydrochloride (C6H5NH2.HCl) in 50 mL of water that had been distilled. Next, extract the ammonium peroxydisulfate (NH4)2S2O2) that diluted in 50 millilitres of distilled water (5.71 g) and 2.59 g, correspondingly. These numbers match up with (0.25M) and (0.3M). Both solutions were kept apart at room temperature (between 18 and 24 °C) for an hour. Subsequently, a magnetic stirring bar was used to rapidly swirl the two solutions in a beaker. The formation of PANI is indicated by the change from colourless to dark green, after which it is permitted to polymerise while at rest. The PANI precipitate was gathered on filter paper the following day, and three 100-mL volumes of acetone and

0.25M hydrochloric acid were used to wash it. After leaving the polymer for a full day (24 hours) to dry in the open, it is combined with PANI powder in a vacuum oven set at 60 degrees Celsius.

3.1. Blending the Doped Solution Utilised

Following the preparation of the Pure PANI solution as previously demonstrated, the Doped PANI solution was created using varying CdO doping ratios (1%, 3%, and 5%). The weight ratios of CdO powder (0.0019, 0.007, and 0.0087 gm) were added to make the CdO solution. The mixture was then individually diluted in 10 ml of solvent DMF and stirred magnetically for two hours.

Following their full dissolution, the pure PANI solution and CdO were combined and left to be prepared separately for five hours employing a magnetic stirrer. The blended solution was then stored in a sanitised glass jar. The following formula is used to determine the percentages of doping in the mixture.

$$W_t\% = \frac{W_{td}}{W_{td} + W} \times 100\% \qquad (1)$$

Where Wt% stands for the doping percentages; t d W is the weight of CdO powder used in this investigation, which is equivalent to 0.0019, 0.007, and 0.0087 gm; and W is the weight of PANI powder used in this investigation, which is 0.18 gm.

3.2. Assessments of Optical Properties

The Shimadzu company produced a double-beam Spectrophotometer (UV-1800) that functioned in the wavelength range of 300-900 nm to evaluate the optical characteristics of the nanofilms deposited on glass slides. The spectroscopic behaviour of a material is used to estimate its optical constants, including its extinction coefficient (k), real and imaginary dielectric constants (ε_r,ε_i) and refractive index (n). To estimate these optical constants, a number of techniques were put forth; these entail evaluation:

3.2.1 Transmission (T)

The transmittance (T) of a material can be calculated as the following: the proportion of the incident ray intensity (I_o) to the transmitting ray intensity (IT) via the medium.

$$T = \frac{I_T}{I_0} \qquad (2)$$

By using the exponential relationship to determine transmittance and absorbance, we may determine (T) as a function of wavelength.

3.2.2 The absorbance (A)

The absorbance (A) is the logarithm of the proportion among the absorbed light intensity (I) and incident light intensity (I0) by the substance. (A) can be ascertained using the relation that follows.

$$A = -Log\, T = Log\left(\frac{I_0}{I}\right) \qquad (3)$$

In this case, I_0 represents the light incident intensity. The intensity of the light absorbed at distance (x) is given by (I).

3.2.3 Reflectivity (R)

The equation (4) can be used to express the reflectance (R), depending on the refractive index value.

$$R = (n-1)^2 + \frac{k^2}{(n+1)^2} + k^2 \qquad (4)$$

According to the law of conservation of energy, (R) can also be determined from the transmission and absorption spectra employing the relation.

3.2.4 Coefficient of Extinction (k)

The imaginary component of the complex refractive index (N*) is represented by the extinction coefficient (k).

$$N^* = n - ik \qquad (5)$$

The accompanying condition (6) gives the genuine part of the complex refractive index (N*), refractive index (n) which relies upon the, crystal structure (grain size), crystal deformities, material sort and, the extinction coefficient (k) and stress in the crystal.

$$k = {}^{\alpha\lambda}/_{4\pi} \qquad (6)$$

Where the incident photon rays' wavelength is represented by λ. (α) Coefficient of absorption

3.2.5 Coefficient of Absorption (α)

The meaning of the absorption coefficient (α) is the material's capacity to retain light of a given wavelength, which can be represented by Lambert-Beer's law utilizing the connection.

$$I = I_0 \exp(-\alpha t) \qquad (7)$$

3.2.6 Index of Refraction (n)

The proportion of light speed in vacuum to that of a medium in ϑ is known as the refractive index (n). The formula (8) can be employed to get the refractive index.

$$n = {}^{c}/_{\vartheta} \qquad (8)$$

The conditions that follow show how the refractive index values were essentially resolved before being entered into an equation taking into account the reflectance and the extinction coefficient, k. Then, the refractive index will be.

3.2.7 Optical Conductivity (σop.)

The primary method used to study a material's optical response is optical conductivity (σop.), which is the electrical conductivity resulting from charge carrier movement caused by the incident electromagnetic waves' alternating electric field (σop.) can be written using the equation that follows.

$$\sigma_{op.} = {}^{\alpha nc}/_{4\pi} \qquad (9)$$

3.2.8 Transitions of Electrons

It is discovered that the Tauc's relation governs the photon absorption in a variety of amorphous materials.

$$\alpha h\vartheta = B(h\vartheta - E_g)^r \qquad (10)$$

In addition to being an identical term for the disorder parameter that is basically free of the photon energy boundary, υ is the radiation recurrence, hυ is the incident photon energy, B is a constant extent with the opposite of amorphousness, α is the absorption coefficient, and Eg is the optical band gap. According to the kind of electronic change, index r addresses the framework of the optical advancement.

At the point when an electron goes from the valence band (V.B) to the conduction band (C.B) with a similar wave vector (k), that is, (Δk=0), and energy is rationed, the progress is alluded to as immediate.

Regardless of whether the electrons moved from V.B. to C.B. at a similar wave vector (k) yet ($\Delta k \neq 0$), the progress is referred to as roundabout since force and energy should be preserved with phonon assistance.

3.3. Nanofilms of Synthesis

After clean samples were used, material was deposited on glass pieces to create nanofilms, which were then sedimented using a spin coating technique. The nanofilm thicknesses that are prepared for this investigation are 68, 46, 44, and 41 nm, and the spinning times are 30 seconds. The spinning speeds for pure PANI and doped PANI by ratios of CdO are 3000, 3500, 4000, and 4500 rpm, respectively. The produced nanofilms underwent heat treatment by being left at room temperature for roughly 24 hours to dry. Nonetheless, there are a number of techniques for determining the film's thickness, including weight, optical, electrical, and other techniques. The technique we used to determine the thickness of the nanofilms in our work is known as optical thin film measurement since it involves the use of an electronic measuring instrument. Lambda (LIMF-10) is the measurement system utilised in this procedure; it is simple to set up and the software is user-friendly. It can be disassembled for purely spectroscopic usage or connected to your microscope to decrease the spot size, making it appropriate for both desktop measuring and online manufacturing. Without GR, the PANI solution is green (an acidic solution); when CdO was added, the solution's colour changed from green to dark green.

4. RESULTS AND DISCUSSION

4.1 Fourier Transformer-Infrared Spectroscopy (FT-IR)

Using infrared spectroscopy, the newly produced PANI/CdO nanofilms were discovered. The samples were collected around 4000 and 400 cm-1 in wavelength. The FT-IR spectra of PANI/CdO nanofilms and PANI that were synthesised at various CdO concentrations (1% and 5%) were discovered during this experiment. PANI is characterised by broad peaks that fall between 3121.75 and 3508.77 cm-1, which relate to the N–H stretching vibrations of secondary amine. Sharp peaks are found at 1504.71 and 1564.43 cm-1 (C=C stretching vibration of benzenoid ring (N-B-N)), 1333.18 and 1387.18 (C - N stretching of secondary aromatic ring), 1651.32 cm-1 (C=C stretching vibration of quinoid ring (N=Q=N)), 1221.18 cm-1 (Aromatic C–H in-plane bending vibrations), 722.32, 828.34, and 913.21 The PANI function groupings concur with [34]. It is evident from these numbers that there is a change in the emission intensity, with each bond's intensity changing accordingly. However, there is no discernible shift in the bond positions.

4.2 The transmittance (T), reflection (R) and absorption (A) spectra of PANI/CdO blend nano composite films and pure PANI films are presented

Figure (1) shows the UV-VIS absorbance spectra for tests of pure PANI combined and PANI/CdO nanocomposite films at different CdO doping proportions (1% and 5%). Both a more sensitive absorption peak at 385 nm and the electron progress from the valance band (V.B), or highest occupied molecular orbital (HOMO), to the conduction band (C.B), or lowest unoccupied molecular orbital (LUMO), which corresponds with the π band $\rightarrow\pi^*$band electronic change of the PANI benzenoid ring, should be prominently displayed in the UV-visible spectrum of the pure PANI blended nanofilm. In the meantime, the shift of the benzenoid ring from a π^* band to a quinoid ring is connected to the second broad assimilation peak at 452 nm. These peaks are associated with the charge transfer between the benzenoid and quinonoid rings as well as the change from (V.B) to (C.B). This is a result of unbound nonbonding electrons, which can ingest radiation with generally low energy. The absorption groups that were removed from the UV-visible spectra relate well with the writing's reports [35].

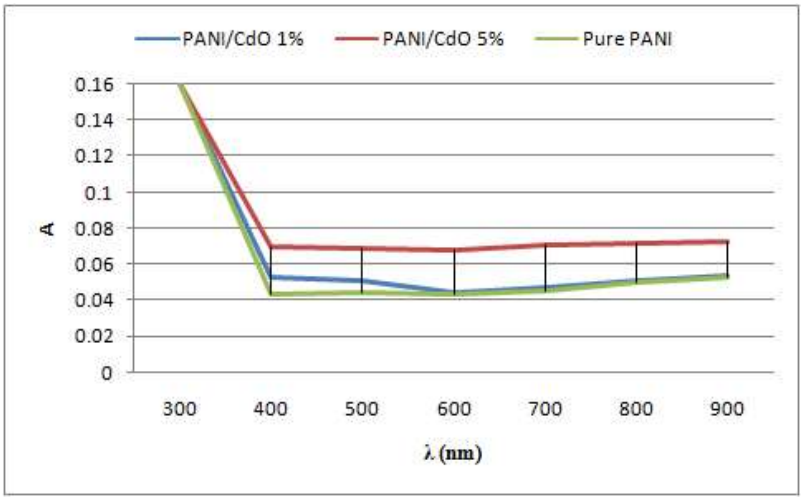

Figure 1: Absorption spectra of PANI/CdO nano composite films and pure PANI as a function of wave length

The PANI/CdO nano composite films' UV-visible spectra at different CdO focuses (1% and 5%) are like those of PANI, and no detectable distinction was found when contrasted with the UV-visible range of the blended pure PANI nano film. The growing CdO grouping, the PANI particles' collaboration with CdO, and the existence of hydrogen particles in the doped PANI (from dopant protonation) could all be contributing factors to the red shift, or movement of the absorption peaks along a higher wavelength side. This peak shifting, which is consistent with [36], shows a narrowing of the optical band gap in the doped films. According to the Beer Lambert law, absorption is directly proportional to the quantity of absorbing particles. The figure shows that as wavelength increased for pure PANI blended and PANI/CdO nano composite films, assimilation spectra decreased, but absorption increased as CdO fixation increased. This is also consistent with previous research that shows absorption to be positively correlated with doping ratio. Figure 2 displays the optical transmission spectra of PANI pure and PANI/CdO nano composite films at various CdO concentrations. This graphic demonstrates how the transmittance intensity rises with wavelength and falls with increasing CdO concentration in the transmittance. This behaviour is caused by the covalent connections that form between polymer chains and additives, which reduce incident light transmission, particularly at the shortest wavelengths.

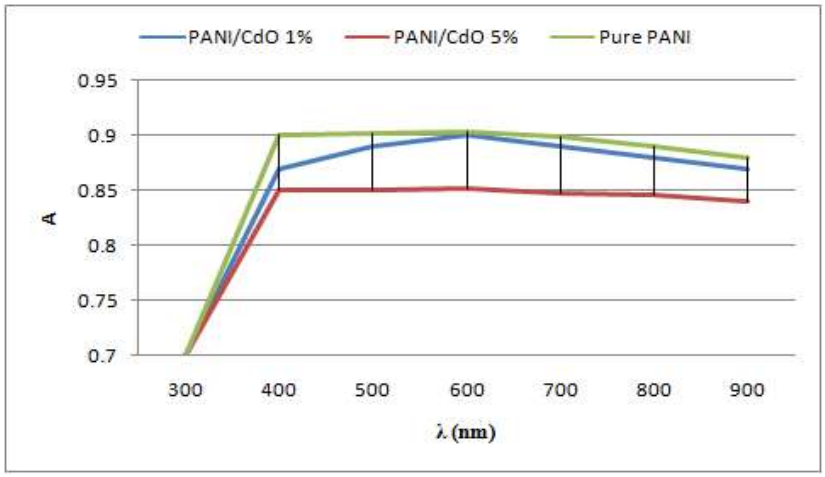

Figure 2: Transmission spectra for pure PANI and PANI/CdO Nano composite films as a function of wave length

After ascending to higher energy levels, the electrons in the outer orbits took up empty spaces in energy bands. As a result, some incident light does not get through. Furthermore, a decrease in light scattering losses results from a decrease in transmittance as the concentration of CdO in the blend increases. The link among wavelength and reflectance is seen in Figure 3. The reflectance rises with increasing CdO concentration since the grain size, crystalline and average surface roughness defects for all nanofilms—both synthesised doped PANI and pure PANI—rose with increasing doping ratio.

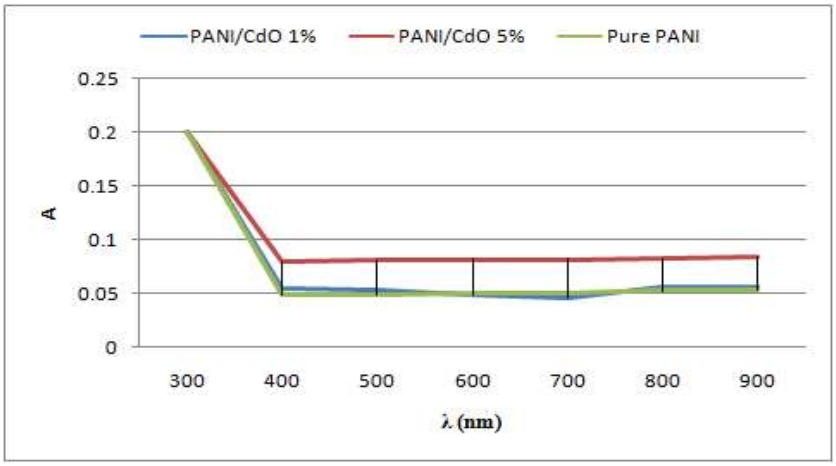

Figure 3: Reflectance spectra for PANI/CdO Nano composite films and pure PANI films as a function of wave length

4.3 PANI/CdO Nanofilms' and pure PANI Absorption Coefficient Spectra

To find the absorption coefficient α(cm-1), use equation (3). In Figure (4), the α(cm-1) for each generated nano composite film is displayed as a function of wavelength. The findings demonstrated that in the visible spectrum, the values of α for PANI/CdO nano composite films and pure PANI films are found to be greater than 104 cm-1. This implies that a direct optical energy gap has been allowed in all of the nano composite films, which explains why ½ is the value of r in equation (10).

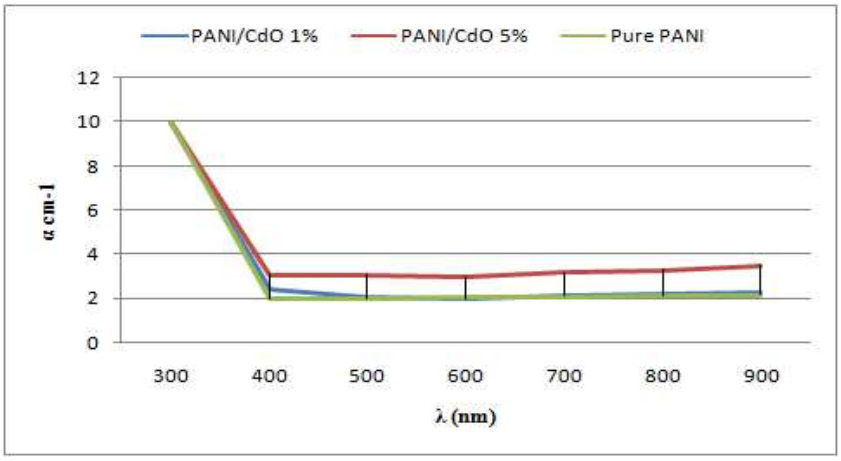

Figure 4: The absorbance coefficient change with wavelength for PANI/CdO nanocomposite films and pure PANI

4.4 The Refractive Coefficient Spectra of PANI/CdO Nano Composite and Pure PANI materials

The values of the refractive coefficient (n) for pure PANI and PANI/GR nanocomposite films as a function of wavelength (λ) are depict in Figure 5. It is found that for all nano composite films with

rising doping ratio concentrations, both the values of (n) growing and reducing with increasing wavelength. The phenomenon makes sense because, in general, strengthening C-H bonds increases n; increasing CdO, on the other hand, enhances the light's propagation velocity across them.

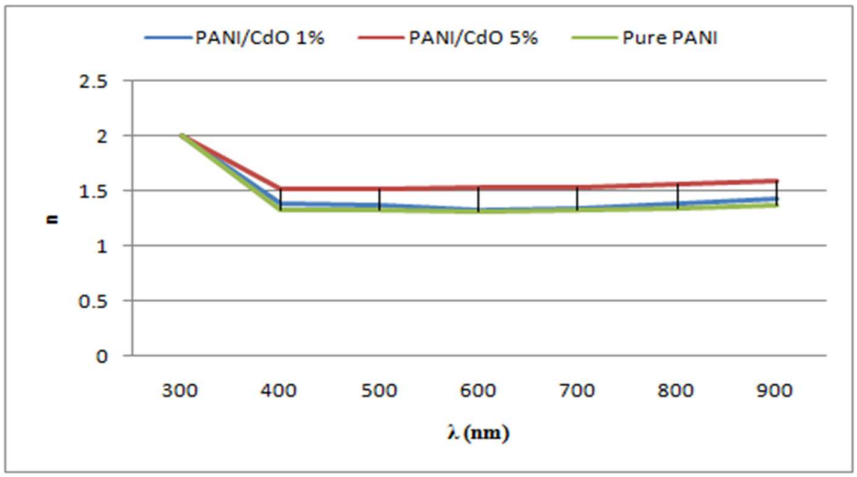

Figure 5: The refractive coefficient fluctuation with wavelength for PANI/CdO nanocomposite films and pure PANI films

4.5 The extinction coefficient spectra of PANI/CdO and pure PANI nanofilms are presented

Equation (6) is used to find the extinction coefficient (k). Figure (6) depicts the connection among (k) and wavelength of the nanocomposite films. It is clear that (k) increased as the proportion of CdO doping rose. This is consistent with [37] and may be explained by the high absorption coefficient and greater ability to absorb a portion of the incident light.

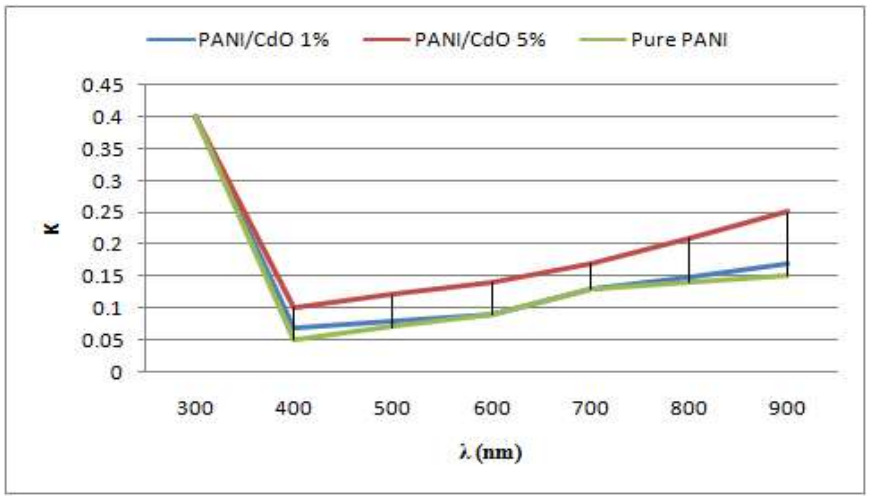

Figure 6: Extinction coefficient change with wavelength for PANI/CdO nanocomposite films and pure PANI

4.6 The purity of PANI and PANI/CdO nanofilms' optical conductivity

Equation (9), when applied, yields the optical conductivity (σop.).As CdO doping percentages increased, a rise in optical conductivity was noted. This could be because of a rise in the contribution of electron transitions between the valence and conduction bands, which reduce the energy gap as an outcome of the development of the sat level.

4.7 Gap in Optical Energy

The formula (10) with r = 1/2 was used to compute the direct optical energy gap (Eg). The energy gap Eg is determined utilizing the Tauce connection and the trial information. Specifically, Eg is obtained by extending the linear segment of the graph at the hυ pivot to the value $(\alpha h\nu)^2 = 0$. The photon energy (hυ) is shown against the graph $(\alpha h\upsilon)^2$. The created nanofilms were found to have an immediate energy gap, and Table 1 records the upsides of Eg for the PANI/CdO (1% and 5%) and pure PANI integrated nano composite films.

Table 1: Eg (e_v) values for films made of PANI/CdO Nano composite and pure PANI synthesised

Compound	Eg (e_v)
PANI/CdO 1%	4.20
PANI/CdO 5%	4.12
Pure PANI	4.41

Figure 7 shows the allowed direct energy gap as a function of the different CdO weight ratios. The graph shows that an increase in weight rate of doping (CdO) results in a decrease in the energy gap and an increase in conductivity. This is because doping generates new levels in the band gap called polaron states, which increase as doping levels do. The band gap decreases as a result of the electrons' smoother transition from the highest occupied energy level in the VB to these local levels in the lowest occupied energy level in the CB.

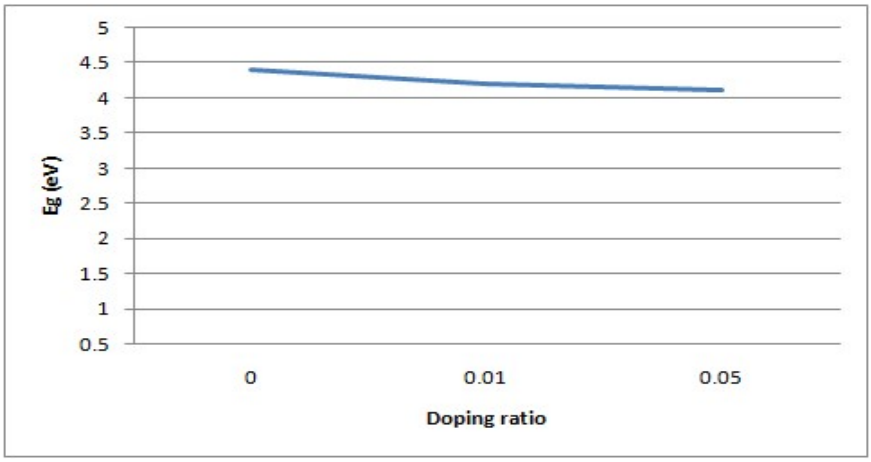

Figure 7: The change in Eg (ev) with respect to CdO doping ratio for both pure PANI and PANI/CdO

5. CONCLUSION

CdO nanoparticles were effectively created using a straightforward sol-gel method. Chemical oxidation polymerisation has been used to create a number of PANI/CdO nanocomposites. In conclusion, a chemical polymerisation process has been effectively used to create PANI homopolymer and PANI/CdO nanocomposites.The study reveals that the addition of CdO to PANI polymer causes this polymer to exhibit a continual change in their physical characteristics (optical).Pure PANI synthesised has a larger optical band gap than (PANI/CdO) nano composite. The measurement of the optical energy gap and other optical parameters, including the dielectric constant and refractive index, is highly dependent on the wavelength of light and the various CdO doping ratios. All samples have allowed direct optical energy gaps, and the electronic transition in pure PANI synthesised and PANI/CdO nanocomposite materials demonstrated direct allowed transition. For pure PANI synthesised

nanofilms, the highest optical energy gap value is approximately 4.41 eV, and when the content of CdO in the nanocomposite samples increases, the value decreases within the range of 4.41 – 4.12 eV.

REFERENCE

1. Zhang, T., Cheng, Q., Jiang, B., & Huang, Y. (2020). Design of the novel polyaniline/polysiloxane flexible nanocomposite film and its application in gas sensor. *Composites Part B: Engineering*, *196*, 108131.
2. Lotfy, S., Atta, A., & Abdeltwab, E. (2018). Comparative study of gamma and ion beam irradiation of polymeric nanocomposite on electrical conductivity. *Journal of Applied Polymer Science*, *135*(15), 46146.
3. Shandilya, M., Thakur, S., & Thakur, S. (2020). Magnetic amendment in the fabrication of environment friendly and biodegradable iron oxide/ethyl cellulose nanocomposite membrane via electrospinning. *Cellulose*, *27*, 10007-10017.
4. Chen, B., Sun, Q., Wang, D., Zeng, X. F., Wang, J. X., & Chen, J. F. (2020). High-gravity-assisted synthesis of surfactant-free transparent dispersions of monodispersed MgAl-LDH nanoparticles. *Industrial & Engineering Chemistry Research*, *59*(7), 2960-2967.
5. Elashmawi, I. S., & Menazea, A. A. (2019). Different time's Nd: YAG laser-irradiated PVA/Ag nanocomposites: structural, optical, and electrical characterization. *Journal of Materials Research and Technology*, *8*(2), 1944-1951.
6. Sharma, A., Sharma, S., Mphahlele-Makgwane, M. M., Mittal, A., Kumari, K., & Kumar, N. (2023). Polyaniline modified Cu2+-Bi2O3 nanoparticles: Preparation and photocatalytic activity for Rhodamine B degradation. *Journal of Molecular Structure*, *1271*, 134110.
7. Ramakoti, I. S., Panda, A. K., & Gouda, N. (2023). A brief review on polymer nanocomposites: current trends and prospects. *Journal of Polymer Engineering*, *43*(8), 651-679.
8. El-Khiyami, S. S., Ismail, A. M., & Hafez, R. S. (2021). Characterization, optical and conductivity study of nickel oxide based nanocomposites of polystyrene. *Journal of Inorganic and Organometallic Polymers and Materials*, *31*(11), 4313-4325.
9. Tajik, S., Beitollahi, H., Nejad, F. G., Shoaie, I. S., Khalilzadeh, M. A., Asl, M. S., ... & Shokouhimehr, M. (2020). Recent developments in conducting polymers: Applications for electrochemistry. *RSC advances*, *10*(62), 37834-37856.
10. Raza, S., Li, X., Soyekwo, F., Liao, D., Xiang, Y., & Liu, C. (2021). A comprehensive overview of common conducting polymer-based nanocomposites; Recent advances in design and applications. *European Polymer Journal*, *160*, 110773.
11. Babazadeh, M., Zalloi, F., & Olad, A. (2015). Fabrication of conductive polyaniline nanocomposites based on silica nanoparticles via in-situ chemical oxidative polymerization technique. *Synthesis and Reactivity in Inorganic, Metal-Organic, and Nano-Metal Chemistry*, *45*(1), 86-91.
12. Imer, A. G. (2016). Investigation of Al doping concentration effect on the structural and optical properties of the nanostructured CdO thin film. *Superlattices and Microstructures*, *92*, 278-284.
13. Noorunisha, T., Nagarethinam, V. S., Suganya, M., Praba, D., Ilangovan, S., Usharani, K., & Balu, A. R. (2016). Doping concentration and annealing temperature effects on the properties of nanostructured ternary CdZnO thin films towards optoelectronic applications. *Optik*, *127*(5), 2822-2829.
14. Poddar, A. K., Patel, S. S., & Patel, H. D. (2021). Synthesis, characterization and applications of conductive polymers: A brief review. *Polymers for Advanced Technologies*, *32*(12), 4616-4641.

15. Das, M., & Sarker, A. K. (2020). Multilayer engineering of polyaniline and reduced graphene oxide thin films on a plastic substrate for flexible optoelectronic applications using NIR. *Russian Journal of Applied Chemistry*, *93*, 1561-1570.
16. Nazari, H., & Arefinia, R. (2019). An investigation into the relationship between the electrical conductivity and particle size of polyaniline in nano scale. *International Journal of Polymer Analysis and Characterization*, *24*(2), 178-190.
17. Rathore, K., & Loonker, S. (2017). Synthesis, characterization and swelling behaviour of guar gum-g-poly (methyl methacrylate) superabsorbent nanocomposite. *Asian Journal of Chemical Sciences*, *2*(1), 1-13.
18. Bazeera, A. Z., & Amrin, M. I. (2017). Synthesis and characterization of barium oxide nanoparticles. *IOSR J. Appl. Phys*, *1*, 76-80.
19. Mezan, S. O., Hello, K. M., Jabbar, A. H., Hamzah, M. Q., Tuama, A. N., Roslan, M. S., & Agam, M. A. (2020). Synthesis and characterization of enhanced polyaniline nanoparticles by oxidizing polymerization. *Solid State Technology*, *63*(1), 256-266.
20. Parekh, Z. R., Chaki, S. H., Hirpara, A. B., Patel, G. H., Kannaujiya, R. M., Khimani, A. J., & Deshpande, M. P. (2021). CuO nanoparticles–synthesis by wet precipitation technique and its characterization. *Physica B: Condensed Matter*, *610*, 412950.
21. Fang, Y., Jayasuriya, D., Furniss, D., Tang, Z. Q., Sojka, Ł., Markos, C., ... & Benson, T. M. (2017). Determining the refractive index dispersion and thickness of hot-pressed chalcogenide thin films from an improved Swanepoel method. *Optical and Quantum Electronics*, *49*, 1-19.
22. Aly, K. A. (2023). Swanepoel method for estimating the film thickness and complex index of refraction by using only the lower envelope: Special case. *Materials Chemistry and Physics*, *310*, 128458.
23. Philip, A., & Kumar, A. R. (2022). The performance enhancement of surface plasmon resonance optical sensors using nanomaterials: A review. *Coordination Chemistry Reviews*, *458*, 214424.
24. Bhadra, J., Alkareem, A., & Al-Thani, N. (2020). A review of advances in the preparation and application of polyaniline based thermoset blends and composites. *Journal of Polymer Research*, *27*(5), 122.
25. Gómez, I. J., Vázquez Sulleiro, M., Mantione, D., & Alegret, N. (2021). Carbon nanomaterials embedded in conductive polymers: A state of the art. *Polymers*, *13*(5), 745.
26. Brachetti-Sibaja, S. B., Palma-Ramírez, D., Torres-Huerta, A. M., Domínguez-Crespo, M. A., Dorantes-Rosales, H. J., Rodríguez-Salazar, A. E., & Ramírez-Meneses, E. (2021). Cvd conditions for mwcnts production and their effects on the optical and electrical properties of ppy/mwcnts, pani/mwcnts nanocomposites by in situ electropolymerization. *Polymers*, *13*(3), 351.
27. Liao, G. (2018). Green preparation of sulfonated polystyrene/polyaniline/silver composites with enhanced anticorrosive properties. *Int. J. Chem*, *10*, 81.
28. Sun, E., Liao, G., Zhang, Q., Qu, P., Wu, G., Xu, Y., ... & Huang, H. (2018). Green preparation of straw fiber reinforced hydrolyzed soy protein isolate/urea/formaldehyde composites for biocomposite flower pots application. *Materials*, *11*(9), 1695.
29. Li, Q., Liao, G., Tian, J., & Xu, Z. (2018). Preparation of novel fluorinated copolyimide/amine-functionalized sepia eumelanin nanocomposites with enhanced mechanical, thermal, and UV-shielding properties. *Macromolecular Materials and Engineering*, *303*(2), 1700407.
30. Nazir, A., Yu, H., Wang, L., Haroon, M., Ullah, R. S., Fahad, S., ... & Usman, M. (2018). Recent progress in the modification of carbon materials and their application in composites for electromagnetic interference shielding. *Journal of materials science*, *53*, 8699-8719.

31. Kenry, & Liu, B. (2018). Recent advances in biodegradable conducting polymers and their biomedical applications. *Biomacromolecules*, *19*(6), 1783-1803.
32. Narasimhachar, R., Basavaraj, B., Vijaykumar, B. T., & Sannakki, B. (2023). Studies on the electrical properties of polyaniline with cadmium oxide nanocomposites. *Materials Today: Proceedings*, *92*, 1676-1680.
33. Abdullah, E. T., Ahmed, R. S., Hassan, S. M., & Naje, A. N. (2015). Synthesis and characterization of PANI and polyaniline/multi walled carbon nanotube composite. *Int. J. Application or Innovation Eng. Mgt*, *4*(9), 130-134.
34. Bachhav, S. G., & Patil, D. R. (2015). Synthesis and characterization of polyaniline-multiwalled carbon nanotube nanocomposites and its electrical percolation behavior. *Am J Mater Sci*, *5*(4), 90-95.
35. Abid Hubeatir, K., Kamil, F., Al-Amiery, A. A., Kadhum, A. A. H., & Mohamad, A. B. (2017). Polymer solar cells with enhanced power conversion efficiency using nanomaterials and laser techniques. *Materials technology*, *32*(5), 279-298.
36. Fakher Alfahed, R. K., Al-Asadi, A. S., Badran, H. A., & Ajeel, K. I. (2019). Structural, morphological, and Z-scan technique for a temperature-controllable chemical reaction synthesis of zinc sulfide nanoparticles. *Applied Physics B*, *125*, 1-11.
37. Muhmood, A. A., Zgair, I. A., Hussein, M. A., Mahdi, L. H., Jabbar, B. S., & Alkhayatt, A. H. O. (2021, May). Preparation and optical characterizations of PVA: Ag Nano composite. In *Journal of Physics: Conference Series* (Vol. 1879, No. 3, p. 032083). IOP Publishing.